View metadata, citation and similar papers at core.ac.uk

brought to you by CORE

provided by Elsevier - Publisher Connector

Earth and Planetary Science Letters 394 (2014) 30–37

Contents lists available at ScienceDirect

Earth and Planetary Science Letters

www.elsevier.com/locate/epsl

Time-capsule concretions: Unlocking burial diagenetic processes in the Mancos Shale using carbonate clumped isotopes

Annabel Dale [a,*], Cédric M. John [a], Peter S. Mozley [b], P. C. Smalley [c], Ann H. Muggeridge [a]

[a] Department of Earth Science and Engineering, Imperial College London, SW7 2BP, UK
[b] Department of Earth and Environmental Science, New Mexico Tech, Socorro, NM 87801, USA
[c] BP Exploration & Production, Chertsey Road, Sunbury-on-Thames, Middlesex TW16 7BP, UK

ARTICLE INFO

Article history:
Received 6 December 2013
Received in revised form 28 February 2014
Accepted 3 March 2014
Available online 1 April 2014
Editor: G.M. Henderson

Keywords:
clumped isotopes
concretion
septarian
clastic
diagenesis

ABSTRACT

Septarian carbonate concretions contain carbonate precipitated during progressive growth of the concretion and subsequent fracture-filling. As such, they have been used to track variations in $\delta^{13}C$ and $\delta^{18}O$ of pore waters during diagenesis and to define diagenetic zones in clastic rocks. However, the $\delta^{18}O$ value of the carbonate is dependent on precipitation temperature and the $\delta^{18}O$ value of the pore fluid from which it precipitated. Interpretations must assume one of these parameters, both of which are highly variable through time in diagenetic settings. Carbonate clumped isotopes of the cement can provide independent estimates of temperature of precipitation, allowing the pore-water $\delta^{18}O$ to be back-calculated. Here, we use this technique on carbonate concretions and fracture fills of the Upper Cretaceous Prairie Canyon Member, Mancos Shale, Colorado. We sampled concretions from two permeable horizons separated by a 5 m shale layer, with one permeable horizon containing concretions with septarian fractures. We show cores precipitated at cooler temperatures (31 °C, ~660 m burial depth) than the rims (68 °C (~1980 m burial depth) and relate that to the $\delta^{13}C_{carbonate}$ values to suggest the concretion core precipitated in the methanogenic zone, with increasing input from thermogenically produced CO_2. The two concretion-bearing horizons have different back-calculated $\delta^{18}O_{porewater}$ values (mean −2.65‰ and 1.13‰ VSMOW) for cements formed at the same temperature and similar $\delta^{13}C$ values, suggesting the shale layer present between the two horizons acted as a barrier to fluid mixing. Additionally, the $\delta^{18}O_{carbonate}$ of the septarian fractures (−13.8‰ VPBD) are due to precipitation at high temperatures (102 to 115 °C) from a fluid with a mean $\delta^{18}O_{porewater}$ of 0.32‰ (VSMOW). Therefore, we can tie in the cementation history of the formation to temporal and spatial variations in $\delta^{18}O_{porewater}$.

© 2014 The Authors. Published by Elsevier B.V. This is an open access article under the CC BY license (http://creativecommons.org/licenses/by/3.0/).

1. Introduction

Carbonate concretions and their internal septarian fracture fills have played an essential role in developing our understanding of clastic rock diagenesis. They can act as 'time-capsules', recording change in the geochemical environment and temperature through progressive carbonate precipitation during burial (e.g. Irwin et al., 1977; Mozley and Burns, 1993; Coniglio et al., 2000; Raiswell and Fisher, 2000; Hudson et al., 2001; Scasso and Kiessling, 2001; McBride et al., 2003; Mozley and Davis, 2005). As such, they are valuable indicators of the timing of diagenetic processes during burial and are often used to infer fluid histories in basins (Machemer and Hutcheon, 1988; Thyne and Boles, 1989; Coniglio et al., 2000; Hudson et al., 2001; Balsamo et al., 2012).

One outstanding question concerns the cause of the $\delta^{18}O$ depletion (relative to carbonate in equilibrium with coeval seawater $\delta^{18}O$) commonly observed in concretions and their septarian fractures fills. There are three principal hypotheses explaining low $\delta^{18}O$ within concretions; precipitation of the carbonate at higher temperatures during burial (Mozley, 1996; Klein et al., 1999; Raiswell and Fisher, 2000), an influx of ^{18}O-depleted fluid at shallow depths (Machemer and Hutcheon, 1988; Thyne and Boles, 1989; Coniglio et al., 2000; Hudson et al., 2001; Balsamo et al., 2012), or a combination of both. The solution to this problem has significant implications for interpretations of the growth environment of concretions, and therefore any interpretations concerning the fluid history in the basin. Using standard isotopic techniques it has been almost impossible to separate whether the ^{18}O-depleted values are due to the involvement of meteoric fluids or precipitation at elevated temperatures, because $\delta^{18}O_{carbonate}$ is dependent on both temperature and the parent $\delta^{18}O_{fluid}$.

* Corresponding author. Tel.: +44 207 594713.
E-mail address: annabel.dale07@imperial.ac.uk (A. Dale).

http://dx.doi.org/10.1016/j.epsl.2014.03.004
0012-821X/© 2014 The Authors. Published by Elsevier B.V. This is an open access article under the CC BY license (http://creativecommons.org/licenses/by/3.0/).

Another outstanding question concerns the transition from microbial to thermal decomposition of organic matter and how this can be determined from geochemical studies of clastic-hosted carbonate concretions (Irwin et al., 1977). If the temperature and by extension relative timing of the concretion precipitation can be constrained, the $\delta^{13}C$ can be correlated with mechanisms of organic matter decomposition in different clastic diagenetic regimes.

Here, we apply a relatively new technique, carbonate clumped isotope thermometry, to derive the temperature, $\delta^{18}O$ and $\delta^{13}C$ isotopic compositions of the precipitating fluid. Recent work has shown the effectiveness of using clumped isotopes to constrain diagenetic processes in carbonates and fault cementation (Huntington et al., 2011; Swanson et al., 2012; Bergman et al., 2013; Budd et al., 2013). Additionally, Loyd et al. (2012) demonstrated for the first time the application to concretions in order to calculate the parent fluid $\delta^{18}O$, proving the use of the technique on concretions and back-calculating the $\delta^{18}O_{fluid}$ they precipitated from. We build on these previous works by examining the temporal variation in $\delta^{13}C$, $\delta^{18}O$ and temperature during diagenesis as recorded by concretions in the Upper Cretaceous Prairie Canyon Member of the Mancos Shale, Colorado. We also investigate the parent fluid $\delta^{18}O$ of septarian fracture fills found within the concretions themselves, the relative timing of which is poorly understood (Mozley, 1996). Our work demonstrates that this approach greatly reduces uncertainties in interpreting the record of carbonate concretions, and increases our ability to accurately constrain timing and mechanisms of chemical changes occurring during diagenesis in clastic rocks.

2. Background

2.1. Geological setting

The samples used in this study came from concretions in the Prairie Canyon Member of the Mancos Shale, which crops out on the southern edge of the Piceance Basin (39°19.062′N; −108°59.011′W). The Prairie Canyon Member is 306 m thick and interpreted as a proximal shoreface deposit, consisting of four coarsening upwards sequences capped by flooding surfaces below which concretionary horizons occur (Cole et al., 1997; Hampson et al., 1999). These concretions are formed of two phases of matrix cement, a Ferroan dolomite and smaller amounts of a Fe-poor dolomite (Klein et al., 1999). They contain calcite septarian fractures that are concentrated at the concretion center and taper off towards the edge forming 'septa' cross cutting the concretion matrix (Astin, 1986).

The concretions and their associated septarian fractures have already been the subject of extensive stratigraphic, carbon and oxygen isotopic and petrographic studies (described in Cole et al., 1997; Hampson et al., 1999; Klein et al., 1999) but their burial history, the source of the pore water from which the cements precipitated and the temperature of formation are still uncertain. Vitrinite reflectance values from Mancos Shale outcrops in the same area range from Rm = 0.42 to 0.68 (Johnson and Nuccio, 1993) and constrain the outcrop to peak burial temperatures of approximately 107 °C using the equation of Barker and Goldstein (1990). However, vitrinite reflectance values are dependent on sample preservation, and the temperature estimates are very sensitive to the specific equation used (Johnson and Nuccio, 1993). The $\delta^{18}O_{carbonate}$ values of the concretions in the Prairie Canyon Member were interpreted as potentially either being precipitated at burial temperatures up to ~92 °C from marine fluids, or in a low-temperature mixed meteoric–marine fluid system (Klein et al., 1999).

2.2. Carbonate clumped isotope thermometry

The carbonate clumped isotope thermometer is based on the abundance of "clumped" ^{13}C–^{18}O bonds within the crystal lattice of a carbonate mineral (Ghosh et al., 2006; Schauble et al., 2006; Eiler, 2007). A sample of the carbonate is reacted with phosphoric acid to produce CO_2, of which the doubly-substituted isotopologue of mass 47 (^{16}O–^{13}C–^{18}O) is of interest. The degree of "clumping" is denoted using the parameter 'Δ_{47}'. Δ_{47} is defined as:

$$\Delta_{47} = 1000\left[\left(R^{47}/R^{47*}\right) - \left(R^{46}/R^{46*}\right) - \left(R^{45}/R^{45*}\right) + 1\right], \quad (1)$$

where R^i = mass i/mass 44 and R^{i*} is the ratio of a gas with the same bulk isotope composition but a stochastic distribution of isotopologues (Eiler, 2007).

The clumping is thermodynamically controlled with an inverse relationship between temperature and abundance of ^{13}C–^{18}O bonds. Furthermore, Δ_{47} does not require any assumptions about the bulk stable isotope composition of the parent fluid (Schauble et al., 2006; Eiler, 2007). With an independent temperature constraint and the $\delta^{18}O_{carbonate}$, the parent $\delta^{18}O_{porewater}$ can be back-calculated and the meteoric–marine mixing vs. temperature hypothesis can be resolved.

3. Material and methods

A total of eight calcite samples from septarian fracture fills and nine dolomite concretion matrix samples were collected from the outcrop (Fig. 1). We used the same two sites, located 1.5 km apart, as Klein et al. (1999). The samples were taken from two cemented horizons, both of which occur at the top of sequence D as described by Cole et al. (1997). The upper horizon has rounded dolomite concretions between 2–3 m in length, and one concretion was sampled here, PC10. The lower horizon, is ~2 m below and more laterally extensive with cement bodies >4 m in length, of which one concretion, PC13 was sampled.

Six septarian fractures were sampled from three separate concretions along the upper horizon in the first area. The other two septarian fracture samples were taken from one concretion (PC12) in the equivalent upper horizon at the second site (Fig. 1). Chips of the fracture fill were collected from six septarian fractures along with two complete fracture fills.

Dolomite matrix samples were taken from two concretions. Three samples were taken from one concretion (PC10) in the upper horizon at the first site. Six dolomite matrix samples were also taken from one larger concretion (PC13) in the lower horizon at the second site (Fig. 1). Klein et al. (1999) mapped out the high resolution spatial distribution of $\delta^{13}C$ and $\delta^{18}O$ for PC10 and PC13, and we reoccupied the same spatial grids (Fig. 2). Hand samples were subsequently powdered using a dental drill prior to analysis.

Two septarian fracture samples were examined in thin section by cathodoluminescence (CL) using a CITL Cathodoluminescence Mk5-2 stage and a Nikon Eclipse 50i microscope with a Nikon DS-Filc camera (see Supplementary material). The CL stage was operated at 15 kV. Thin sections were examined for evidence of alteration through weathering, and none was observed. Five septarian fracture fills were analyzed for phase identification by powder X-ray diffraction at the Natural History Museum, London. This was carried out on a Phillips PW 1830 diffractometer system using Cu Kα radiation at 45 kV and 40 mA. The resulting diffraction pattern was then overlaid with known mineral XRD patterns from the International Centre Diffraction Database (ICDD) for qualitative phase analysis by peak matching.

Isotopic analyses were carried out in the Qatar Stable Isotope Laboratory at Imperial College London. Between 5–8 mg of calcite

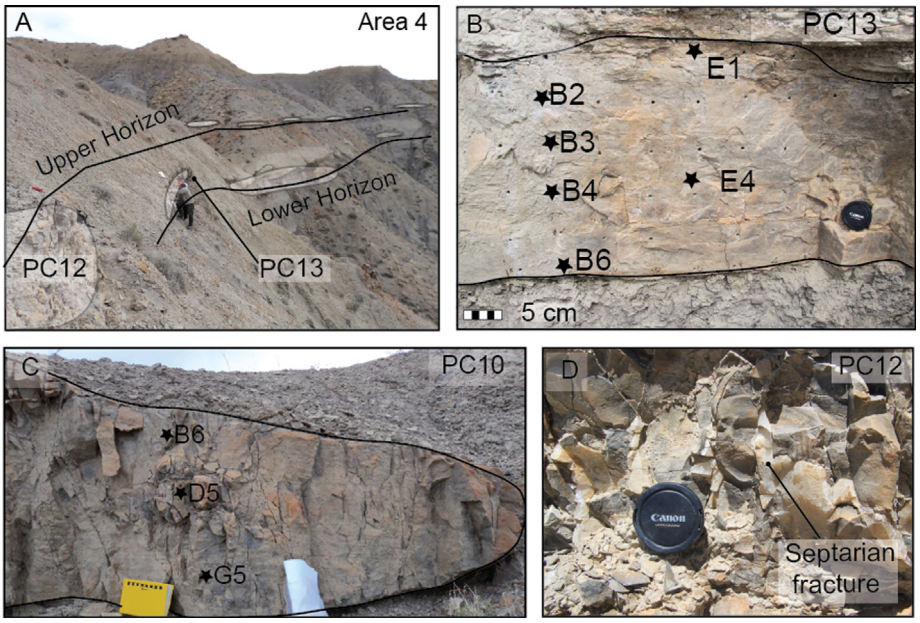

Fig. 1. (A) Upper and lower horizons at Area 4. Septarian fracture samples were taken from PC12. (B) Matrix transect at grid PC13, stars represent drill holes. (C) Matrix transect at Grid PC10. (D) Septarian fractures from concretion PC12.

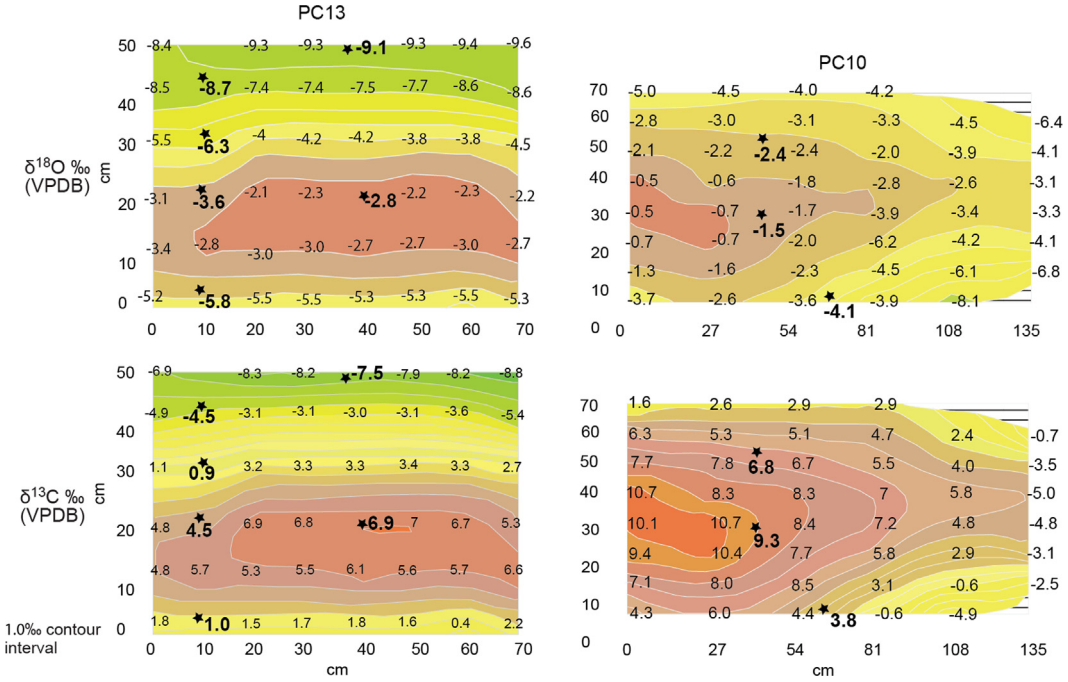

Fig. 2. Grids for PC10 and PC13 used by Klein et al. (1999). Measurements by Klein et al. (1999) are non-bold, isotope values obtained in this study are bold and samples denoted by a star. Contouring is every 1‰, as per Klein et al. (1999). $\delta^{13}C$ and $\delta^{18}O$ values of re-occupied sites fell within 1‰ of those measured by Klein et al. (1999).

from fracture fills were reacted in 104% phosphoric acid at 70 °C for 15 min and the resulting CO_2 gas was purified in a manual vacuum line following Dennis and Schrag (2010). Dolomite matrix samples were first treated with cold 3% H_2O_2 and distilled water rinses to remove organic material (Ferry et al., 2011), and 9–10 mg of sample were reacted at 90 °C for 45 min before being passed through the vacuum line. All samples are reacted online with the CO_2 produced being continually trapped during the reaction. Resultant CO_2 was measured on one of two Thermo Fisher MAT 253 isotope ratio mass spectrometers with an integration time of 2 h (see Huntington et al., 2009). To monitor for contamination, only samples with δ_{48} and Δ_{48} values that fell within 2‰ of the appropriate heated gas line were accepted (Huntington et al., 2011).

The acid fractionation factor of Kim et al. (2007) and the dolomite fractionation factor of Rosenbaum and Sheppard (1986) were used to correct the $\delta^{18}O_{calcite}$ and $\delta^{18}O_{dolomite}$ respectively. Rosenbaum and Sheppard (1986) was used as it was used in a previous study of these cements (Klein et al., 1999). Acid fractionation factors for Δ_{47} are taken from Guo et al. (2009) (equation 23). This was used as it can be adjusted for 70 °C and 90 °C for calcite and dolomite respectively. At 90 °C it gives a fractionation factor of 0.069‰, comparable with recently published empirical fractionation factors for 90 °C of 0.07‰ and 0.076 + 0.007‰

Table 1
Concretion and septarian fracture $\delta^{13}C$, $\delta^{18}O$, Δ_{47} and $\delta^{18}O_{porewater}$.

Sample	Mineralogy	Type[a]	n	$\delta^{13}C$ (VPDB)[b]	$\delta^{18}O_{carbonate}$ (VPDB)[b]	$\Delta47$[c]	T (°C)	$\delta^{18}O_{porewater}$ (VSMOW)[d]
PC10C1SC1	Calcite	F	4	−3.35 (0.04)	−14.35 (0.18)	0.511 ± 0.014	102 ± 8	0.63 ± 1
PC10C1SC2	Calcite	F	3	−3.03 (0.09)	−14.10 (0.03)	0.497 ± 0.004	111 ± 3	0.29 ± 0.33
PC10C1SC3	Calcite	F	4	−3.03 (0.01)	−13.44 (0.05)	0.490 ± 0.010	101 ± 9	−0.09 ± 1.04
PC10C2SC1	Calcite	F	4	−3.03 (0.02)	−13.77 (0.09)	0.512 ± 0.016	115 ± 6	0.91 ± 0.67
PC10C2SC2	Calcite	F	3	−3.08 (0.01)	−13.82 (0.09)	0.499 ± 0.012	110 ± 8	0.38 ± 0.9
PC12SC1 (area 2)	Calcite	F	3	−2.89 (0.01)	−13.72 (0.04)	0.499 ± 0.03	109 ± 2	0.49 ± 0.24
PC12SC3 (area 2)	Calcite	F	3	−3.13 (0.03)	−13.56 (0.08)	0.499 ± 0.012	109 ± 7	0.58 ± 0.79
PC10C5SC2	Calcite	F	3	−2.10 (0.02)	−13.21 (0.25)	0.502 ± 0.013	107 ± 8	0.96 ± 1.09
PC10B6	Dolomite	M	2	6.81 (0.12)	−2.35 (0.12)	0.631 ± 0.009	43 ± 3	0.63 ± 0.65
PC10D5	Dolomite	M	3	9.33 (0.15)	−1.47 (0.27)	0.620 ± 0.005	48 ± 2	2.09 ± 0.59
PC10G5	Dolomite	M	3	3.83 (0.15)	−4.06 (0.48)	0.608 ± 0.012	53 ± 5	0.66 ± 1.28
PC13 B2	Dolomite	M	3	−4.54 (0.21)	−8.7 (0.41)	0.595 ± 0.004	58 ± 1	−3.76 ± 0.55
PC13 B3	Dolomite	M	2	0.90 (0.08)	−6.29 (0.66)	0.612 ± 0.001	51 ± 0	−2.57 ± 0.55
PC13 B4	Dolomite	M	2	4.54 (0.2)	−3.59 (0.19)	0.664 ± 0.015	31 ± 5	−3.15 ± 1.18
PC13 B6	Dolomite	M	3	0.97 (0.04)	−5.76 (0.05)	0.626 ± 0.012	45 ± 4	−2.10 ± 0.89
PC13 E1	Dolomite	M	2	−7.5 (0.07)	−9.1 (0)	0.573 ± 0.011	68 ± 5	−2.5 ± 0.73
PC13 E4	Dolomite	M	3	6.86 (0.05)	−2.28 (0.05)	0.666 ± 0.004	30 ± 1	−1.86 ± 0.3

[a] F = fracture, M = matrix.
[b] Error is 1σ for $\delta^{13}C$ and $\delta^{18}O_{carbonate}$.
[c] Error for Δ_{47} is given as standard error, calculated by the replicate standard deviation divided by square root of n.
[d] Back-calculated using fractionation factors of Vasconcelos et al. (2005) for dolomite and Friedman and O'Neil (1977) for calcite. Error for $\delta^{18}O_{porewater}$ is calculated using 1σ of $\delta^{18}O_{carbonate}$ and temperature standard error.

(Wacker et al., 2013; Henkes et al., 2013). For the dolomite samples reacted at 90 °C, the maximum temperature change caused by different fractionation factors is ∼3 °C, which falls within the standard error of many of the samples (Table 1).

The Δ_{47} values were converted into temperature using Passey and Henkes (2012) (Eq. 5), adjusted to take into account that an acid fractionation factor of 0.081‰ was used by Passey and Henkes (2012). Parent $\delta^{18}O_{porewater}$ values were calculated using calcite–water fractionation factors from Friedman and O'Neil (1977) for calcite and Vasconcelos et al. (2005) for dolomite. The Vasconcelos et al. (2005) was used as it is a low temperature calibration for dolomite, and the concretions can form at low temperatures. Using the higher temperature calibration of Land (1980) to back-calculate $\delta^{18}O_{porewater}$ shifts all the back-calculated pore-water compositions to ∼ 1‰ more negative, but this does not have a major impact on the interpretation of the results.

All Δ_{47} values are reported in the absolute reference frame with the methodology described in Dennis et al. (2011), using standards, including Carrara Marble, an externally verified carbonate standard (ETH-3), heated gases and CO_2 gases equilibrated with water at 25 °C, 50 °C and 80 °C. During the period of measurement on each machine the Carrara Marble standard had a mean Δ_{47} (in the universal reference frame) of 0.391 (1σ $0.034n = 42$) for one machine and 0.410 (1σ $0.02n = 13$) for the other. Both $\delta^{18}O$ and $\delta^{13}C$ values are reported against Vienna PeeDee Belemnite (VPDB), and the $\delta^{18}O_{porewater}$ is reported against Vienna Standard Mean Ocean Water (VSMOW).

4. Results

All results are shown in Table 1. Mean $\delta^{13}C$ and $\delta^{18}O_{carbonate}$ values for the septarian fracture fills are −2.96 (0.37‰ 1σ) and −12.22 (0.36‰ 1σ), respectively. The mean $\delta^{18}O_{porewater}$ composition for the septarian fills is 0.32‰ ± 0.5‰ (1σ). Matrix dolomite cement $\delta^{13}C$ values are increasingly depleted towards the edges of the concretions, and range from positive $\delta^{13}C$ up to 9.33‰ in the core of PC10, to −7.5‰ towards the edge in PC13. The $\delta^{18}O_{carbonate}$ has a similar trend, becoming increasingly depleted towards the edges of the concretions, ranging from −1.47‰ at the center of PC10 to −9.1‰ at the edge of PC13. Results for the matrix samples can be shown overlying those obtained by Klein et al. (1999) in Fig. 2. Back-calculated $\delta^{18}O_{porewater}$ compositions are shown in Fig. 3. The standard deviation reported for the matrix samples (Table 1) likely represents a combination of analytical error and the heterogeneity of the samples, as they are mixed carbonate phases.

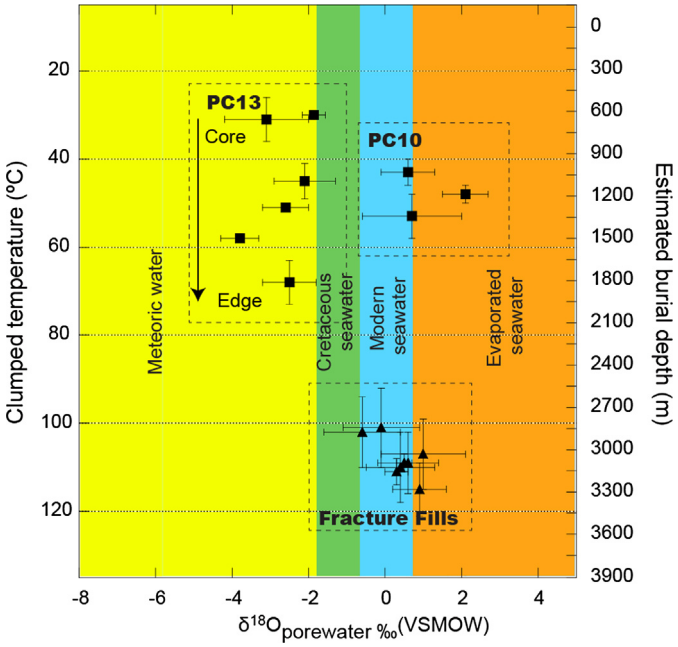

Fig. 3. Burial depth (km) and clumped isotope temperatures (°C) vs. calculated $\delta^{18}O_{porewater}$. Septarian fractures (triangles) and matrix cements (squares) are plotted. Burial depth assuming a geothermal gradient of 30 °C/km and a sea-floor temperature of 15 °C. Error bars are 1 standard error (S.E.).

The mean Δ_{47} for the septarian fracture infills is 0.501 ± 0.02‰ (1σ). For the matrix dolomite there is a core to rind trend in Δ_{47} that corresponds to the changes in $\delta^{13}C_{carbonate}$ and $\delta^{18}O_{carbonate}$. They range from 0.573‰ to 0.666‰. This translates to temperatures of 107–115 °C for the fracture fill, and between 30 ± 1 °C to 68 ± 5 °C for the matrix samples (Table 1).

5. Discussion

5.1. Assessing the integrity of the clumped isotope results

Two main complications can arise when interpreting the $\delta^{18}O$ and Δ_{47} values of the samples. First, the cements may have undergone recrystallization during burial, which could cause an alteration of both the $\delta^{18}O_{carbonate}$ and the Δ_{47} signatures. Second, the Δ_{47} could have been reset in a closed system during burial through solid-state diffusion, a process which can occur whilst the $\delta^{18}O_{carbonate}$ remains unaffected (see Ferry et al., 2011; Quade et al., 2013).

Although we cannot completely rule out recrystallization, we deem it unlikely as (1) we found no petrographic textural evidence of recrystallization in the fracture calcite in thin sections and under cathodoluminescence (see appendix), (2) at least in the dolomite matrix, cooler temperatures are preserved in the center of the concretions (~30 °C), and 3) there is a range of different $\delta^{18}O$ values in the surrounding dolomite matrix, which may have been expected to homogenize with recrystallization. Furthermore, with regards to understanding the basin fluid history, even if recrystallization had occurred, the back-calculated pore fluid should represent the $\delta^{18}O_{porewater}$ composition at the temperature of recrystallization and has less impact on our interpretation.

It also seems unlikely that the dolomite concretion matrix has been reset, given the preservation of low temperatures at the cores of the concretions. For the calcite fracture fills, the likelihood of resetting is a function of the temperatures the Prairie Canyon reached during burial, and the length of time is was held at these temperatures (Dennis and Schrag, 2010; Huntington et al., 2011; Passey and Henkes, 2012). However, previous works on the clumped isotope signatures of diagenetic calcite samples have been show to preserve potentially original, low precipitation temperatures (~24 °C) next to high temperature calcite (137 °C) in fault zones (Swanson et al., 2012), dike intrusion settings (Finnegan et al., 2011), and low temperature 14–19 °C calcite next to 94–123 °C calcite in Eocene gastropod shells (Huntington et al., 2011).

It is difficult to constrain the temperature history of the outcrop independently of the clumped isotope data, and especially the duration of exposure of the concretions to burial temperatures. Vitrinite reflectance data imply a maximum temperature of ~107 °C, although this is likely associated with large uncertainties that are difficult to constrain (Johnson and Nuccio, 1993). The Prairie Canyon Member also appears in wells to the north of the outcrop studied (Nuccio and Roberts, 2003). In these wells it has been exposed to temperatures >100 °C for ~80 million years, so the length of burial of the outcrop examples used in this study is likely to be significantly less than this. Despite the lack of control of the timing, the fracture fills also have back-calculated $\delta^{18}O_{porewater}$ compositions within error of the $\delta^{18}O_{porewater}$ for matrix dolomite cements in the concretion PC10. This is significant, as the fractures are taken from the same horizon as PC10 and had resetting of the Δ_{47} signature occurred, the back-calculated fluids of the fractures and matrix may be expected to be different.

5.2. Growth of the concretions

A simple model of concretion formation is based on 'concentric growth', with progressively younger cement phases growing outwards from the center to the edge of the concretion. However, many concretions form in a pervasive manner, in which early and late stage cements precipitated throughout the concretion body. This can occur where early cementation is incomplete and preserves residual porosity that is protected against compaction (Mozley 1989, 1996; Raiswell and Fisher, 2000). The spatial distribution of $\delta^{13}C$ and $\delta^{18}O$ in the Prairie Canyon concretions could be interpreted as either consistent with the concentric growth model (Mozley et al. 1996; Klein et al., 1999), or a pervasive growth mechanism, where intermediate between the edge and core represent mixtures of early and late cements, with greater amounts of late cements present near the outer edge (Mozley, 1989, 2002) (Fig. 2). In this case it may be difficult to determine whether cements occurring at intermediate locations between a concretion centre and edge are be due to (a) successive generations of cement growing concentrically from the centre, or (b) mixtures of early and late cements where the percent ratio of centre: edge cements in a sample varies according to its relative position. In these concretions, it is difficult to distinguish any core to edge relationship in matrix cement mineralogy (Klein et al., 1999). In scenario (a) the temperatures inferred from Δ_{47} values are the actual temperatures that occurred during the formation of those cements. In scenario (b) the temperatures inferred from Δ_{47} values are not those that occurred during cement formation.

It is not possible to distinguish discrete layers in the concretions in the Prairie Canyon outcrop or thin sections from those concretions. Previous work suggests that although a Fe-poor dolomite preceded a more ferroan dolomite, there is no center-to-edge relationship in abundance of the two (Klein et al., 1999). It is possible that precipitation of a relatively small amount of an early ferroan dolomite phase stabilized the sediment framework and prevented compaction in areas of the concretions (Spinelli et al., 2007), allowing a later, higher temperature ferroan dolomite to precipitate throughout. Thus, there is no way to be certain that the ferroan cement all represents one phase of precipitation. It is likely, however, that even in the case of mixed cements the concretion centre is predominantly early cement and the edge is predominantly late (Mozley 1989, 1996). In this case we assume here that the concretion centre is predominantly early cement and the edge is late. We can determine that in concretion PC13 the cement in the concretion center precipitated at lower temperatures (31 ± 5 °C), whilst cement at the edge precipitated at higher temperatures (68 ± 5 °C) (Fig. 3). Concretion PC10 is significantly smaller than PC13 and shows less variation from core to edge in $\delta^{13}C$ and $\delta^{18}O$ (Fig. 2). However, as the cements most depleted in $\delta^{18}O$ and $\delta^{13}C$ were not sampled to measure Δ_{47}, we cannot be certain of the range in temperature nor when the concretion finished forming.

5.3. Relative timing of burial processes compared to $\delta^{13}C$

By reference to a burial curve estimated for this area for subsurface wells containing the Mancos Shale (Govt. 31-10 well, page 15 in Nuccio and Roberts, 2003) the data from PC13 relates to a depth of approximately ~660 m and age of 75 m.y. for the formation of the concretion centre and a depth of ~1980 m and age of 65 m.y. for the formation of the edge cement, assuming a geothermal gradient of 30 °C/km and seafloor temperature of 15 °C (see Klein et al., 1999 for a discussion of sea-floor temperatures). This would indicate concretion growth lasted 10 million years and occurred over a depth range of ~1400 m. The timing of septarian fracture formation would have been at approximately ~35 m.y. and ~3500 m depth.

These data can be used to help constrain the timing of organic decomposition processes (Fig. 4) as reflected in the $\delta^{13}C$ of the cement. The core of concretion PC13 has a heavy $\delta^{13}C$ signature (6.8‰); such enrichment of pore waters in ^{13}C is typically attributed to methanogenesis (Irwin et al., 1977). The edge cements are more depleted in ^{13}C ($\delta^{13}C = -9.1‰$) probably reflecting the onset of thermocatalytic decarboxylation (Irwin et al., 1977; Klein et al., 1999). The temperature of the concretion core (31 ± 5 °C) is compatible with temperatures (~30 °C) at which methanogenic bacteria have been used to experimentally precipitate stoichiomet-

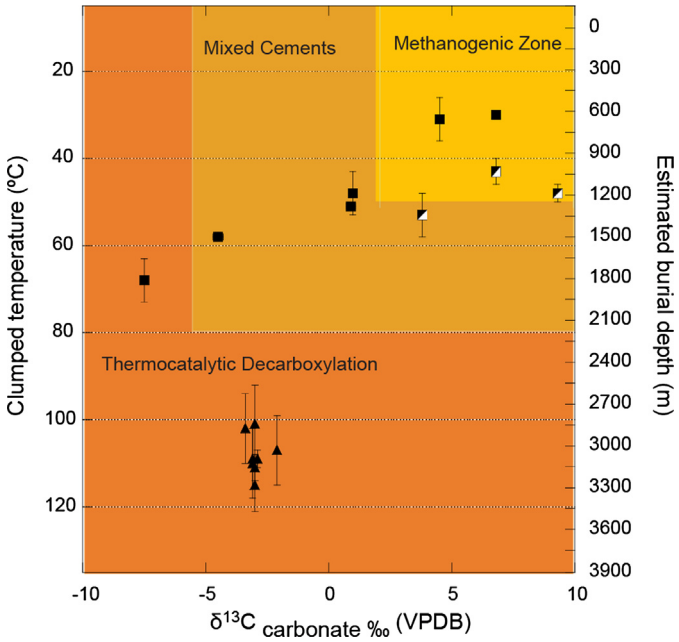

Fig. 4. Change in $\delta^{13}C_{carbonate}$ with temperature and depth. Burial depth assuming a geothermal gradient of 30 °C/km and a sea-floor temperature of 15 °C. Black squares are PC13, half white half black are PC10, triangles are septarian fills. Error bars are standard error (1 S.E.) for temperature and 1σ for $\delta^{13}C$.

ric dolomite (Kenward et al., 2009). The upper temperature limit of bacterial methanogenesis in the Prairie Canyon must be lower than temperatures recorded by cements at the outer rim of the concretion, where $\delta^{13}C$ values of $-7.5‰$ imply thermocatalytic decarboxylation at a temperature of at least 68 ± 5 °C based on clumped isotopes results (Fig. 3).

The final cementation event to occur is the infill of the septarian fractures, of which the mean precipitation temperature is 108 °C (Fig. 3), corresponding to burial depths of ~2.7 to 3.5 km. The mean $\delta^{13}C$ value of the calcite is $-3.3 \pm 0.3‰$ (VPDB), and may reflect thermocatalytic decarboxylation processes, similar to the concretion edge cements of PC13. The texture of the calcite infill does not imply growth during fracture opening, as the crystals show no preferential elongation perpendicular to fracture opening, and as such it is impossible to infer the timing of fracturing except that it is later than the concretion edge cements.

Additionally, this shows that the cooler carbonate clumped isotope temperatures of early dolomite concretion cores are preserved, even when in close spatial proximity to higher temperature dolomite and calcite phases and subjected to burial depths >3.8 km. This implies that the dolomite phase can withstand resetting up to ~115 °C for at least ~40 m.y.

5.4. Parent fluid $\delta^{18}O$ of the concretion matrices

For the matrix dolomite cement, the back-calculated $\delta^{18}O_{porewater}$ values for the core and edge of concretion PC13 are anomalously depleted with values of $-2.5‰$ and $-1.86‰$ respectively. The first of these values is similar to those obtained by Loyd et al. (2012) for concretions in the Holz Shale, which they interpreted to represent meteoric–marine mixing. Given the near-shore geological setting of portions of the Prairie Canyon (Hampson et al., 1999) and the fact that $\delta^{18}O_{porewater}$ values for the edge of PC13 are slightly more negative than the inferred Cretaceous seawater value of $-1.2‰$ (Shackleton and Kennett, 1975; Klein et al., 1999) these data could also suggest a degree of meteoric water influx. The Prairie Canyon Member is sandier and a more permeable horizon than the surrounding Mancos Shale. It may have acted as a coastal aquifer for meteoric water, in a similar manner to the New Jersey Margin off the eastern seaboard of the USA today (Malone et al., 2002). Siliciclastic carbonate concretions are also found in these settings (Malone et al., 2002). There does not appear to be a large difference between the core and edge cement $\delta^{18}O_{porewater}$, implying little change in the $\delta^{18}O$ values of the parent fluid during burial and formation of PC13.

The back-calculated $\delta^{18}O_{porewater}$ of matrix cements from PC10 is up to 2‰ heavier that that of PC13 (Fig. 3). Additionally, although the precipitation of the septarian fracture fills is a much later event in the burial history as demonstrated by higher temperatures of precipitation, the $\delta^{18}O_{porewater}$ is still within the range of error of the earlier concretion matrix cements, with a mean $\delta^{18}O_{porewater}$ of $0.32 \pm 0.5‰$ (1σ) (Fig. 3). This is significant as the matrix cements of PC10 concretions may have precipitated from pore fluids with a heavier $\delta^{18}O_{porewater}$ than PC13, at similar temperatures and $\delta^{13}C$ values. If this were the case, it implies the type of porewater (meteoric/marine) is not an essential control on the precipitation of the carbonate cements and that the septarian fracture fills did not precipitate from meteoric–marine mixed water. Secondly, it may suggest that the two porefluids were not in communication with each other across the 2 m shale layer between them. Finally, the $\delta^{18}O_{porewater}$ within the PC10 layer does not exhibit a major (>1‰) change between the early matrix cementation and the later and deeper fracture fill precipitation.

There are several potential causes of the differences in $\delta^{18}O_{porewater}$ between PC13 horizon and the PC10 concretionary horizon. There may have been an inherent heterogeneity in the original porefluid at time of deposition, potentially due to changes in sedimentation. This hypothesis is supported by a previous sedimentological study by Hampson et al. (1999), who interpreted the shale horizon between the PC10 and PC13 to represent the distal toe of another parasequence. Alternatively, the horizon of PC13 may have been a preferential flow pathway for meteoric–marine mixed fluids to travel through. This is supported by the observation that the extent of cementation in the PC13 horizon is much greater than PC10. An influx of Ca^{2+}, Mg^{2+}, Fe^{2+} and CO_3^{2-} ions from fluids along the horizon could replenish the ion gradient and explain the cementation (Bjorkum and Walderhaug, 1993).

It is also possible that difference in $\delta^{18}O_{porewater}$ between the two horizons is caused by diagenetic processes, such as extended water–rock interaction, or clay dewatering during burial (Clayton et al., 1966). However, the difference is observable at temperatures of 31–40 °C so many higher temperature diagenetic processes, such as clay transformation (temperatures in excess of 100 °C) can be ruled out (Aoyagi and Kazama, 1980). However, volcanic ash, which is present in the Mancos Shale, alters at low temperatures and has been suggested as a mechanism for significant depletion in $^{18}O_{porewater}$ (Lawrence et al., 1979; Lawrence and Gieskes, 1981; Lawrence and Taviani, 1988). Finally, another possible solution may be shale hyperfiltration, which could cause fractionations in $\delta^{18}O$, and a $\delta^{18}O_{porewater}$ up to 0.8‰ lighter on the lower pressure side of the shale layer (Coplen and Hanshaw, 1973).

6. Conclusions

Clumped isotope analysis has been used to analyse the matrix cements of two concretions from two different horizons and septarian fracture fills from four concretions within one of those horizons in the Mancos Shale found in the Prairie Canyon outcrop. Analyses reveal that the concretion matrix in the core of the concretions formed at shallow burial depths (<1 km burial), before later cements at the edge of the concretions precipitated at depths of ~1.5 km. Subsequently, septarian fracture infills formed at depths of ~3 km. The spatial juxtaposition of low temperature dolomite cements and high temperature cements

suggests that it is resistant to at least complete resetting up to ~115 °C over a timescale of at least 40 myrs. The various cement phases record the history of changes in organic matter decomposition via changes in $\delta^{13}C_{carbonate}$, indicating a change from the methanogenic zone at <1 km burial to one influenced by the temperature-driven breakdown of organic matter at >2 km burial. The $\delta^{18}O_{porewater}$ shows that the matrix cements for horizon PC13 precipitated from a porewater with a marine-meteoric mixed signature, whilst horizon PC10 and the associated septarian fracture fills formed from porewaters isotopically enriched in ^{18}O relative to Cretaceous seawater. This may reflect original porewater heterogeneities, differences in horizon permeability or be caused by an early diagenetic process such as alteration of volcanic ash or shale hyperfiltration.

Our data showing high temperature precipitation for the septarian infill from a non-meteoric parent porewater should caution others when using septarian calcite to infer meteoric input through time based only on light oxygen isotopes. Independent verification from other palaeothermometers, such as carbonate clumped isotope thermometry is essential.

Using carbonate clumped isotope thermometry, we demonstrate that septarian (and non-septarian) concretions formed over a wide range of depths and temperatures, constraining the diagenetic processes and pore fluid compositions in formation. This is achieved by providing an independent temperature axis to determine relative timing of cement phases (related to burial temperatures), and by distinguishing between meteoric-mixing or high temperature precipitation of carbonate cements. This warrants a broader use of this technique to further our understanding of processes occurring during clastic diagenesis.

Acknowledgements

This research was funded by a BP and Engineering and Physical Sciences Research Council CASE Studentship (Grant number: EATAS - NN0722); we thank BP for permission to publish. The authors would like to thank Anne-Lise Jourdan, Tobias Kluge, Simon Davis, John MacDonald and Veerle Vandeginste for help in the lab, Gary Hampson for maps, Rex Cole for assistance in the field and Martin Gill for XRD analyses. We would also like to thank Max Coleman two anonymous reviewers and Editor Gideon Henderson whose comments helped to improve this paper,

Appendix A. Supplementary material

Supplementary material related to this article can be found online at http://dx.doi.org/10.1016/j.epsl.2014.03.004.

References

Aoyagi, K., Kazama, T., 1980. Transformational changes of clay minerals, zeolites and silica minerals during diagenesis. Sedimentology 27, 179–188.
Astin, T.R., 1986. Septarian crack formation in carbonate concretions from shales and mudstones. Clay Miner. 21, 617–631.
Balsamo, F., Storti, F., Grocke, D.R., 2012. Fault-related fluid flow history in shallow marine sediments from carbonate concretions, Crotone basin, south Italy. J. Geol. Soc. 169 (5), 613–626.
Barker, C.E., Goldstein, R.H., 1990. Fluid-inclusion technique for determining maximum temperature in calcite and its comparison to the vitrinite reflectance geothermometer. Geology 18 (10), 1003.
Bergman, S.C., Huntington, K.W., Crider, J.G., 2013. Tracing palaeofluid sources using clumped isotope thermometry of diagenetic cements along the Moab Fault, Utah. Am. J. Sci. 313.
Bjorkum, P.A., Walderhaug, O., 1993. Isotopic composition of a calcite cemented layer in the lower Jurassic Bridport Sands, southern England: Implications for formation of laterally extensive calcite-cemented layers. J. Sediment. Petrol. 63, 678–682.
Budd, D.A., Frost, E.L., Huntington, K.W., Allwardt, P.F., 2013. Syndepositional deformation features in high-relief carbonate platforms: Long-lived conduits for diagenetic fluids. J. Sediment. Res. 83 (1), 12–36.
Clayton, R.N., Friedman, I., Graf, D.L., Mayeda, T.K., Meents, W.F., Shimp, N.F., 1966. The origin of saline formation waters. J. Geophys. Res. 71 (16), 3869–3881.
Cole, R., Young, R.G., Willis, G.C., The Prairie Canyon member, a new unit of the Upper Cretaceous Mancos Shale, West-Central Colorado and East-Central Utah, vol. 23. Utah Geological Survey Miscellaneous Publication 97-4.
Coniglio, M., Myrow, P., White, T., 2000. Stable carbon and oxygen isotope evidence of cretaceous sea-level fluctuations recorded in septarian concretions from Pueblo, Colorado, U.S.A. J. Sediment. Res. 70 (3), 700–714.
Coplen, T.B., Hanshaw, B.B., 1973. Ultrafiltration by a compacted clay membran – I. Oxygen and hydrogen isotopic fractionation. Geochim. Cosmochim. Acta 37, 2295–2310.
Dennis, K.J., Schrag, D.P., 2010. Clumped isotope thermometry of carbonatites as an indicator of diagenetic alteration. Geochim. Cosmochim. Acta 74 (14), 4110–4122.
Dennis, K.J., Affek, H.P., Passey, B.H., Schrag, D.P., Eiler, J.M., 2011. Defining an absolute reference frame for 'clumped' isotope studies of CO_2. Geochim. Cosmochim. Acta 75 (22), 7117–7131.
Eiler, J.M., 2007. "Clumped-isotope" geochemistry – The study of naturally-occurring, multiply-substituted isotopologues. Earth Planet. Sci. Lett. 262 (3–4), 309–327.
Ferry, J.M., Passey, B.H., Vasconcelos, C., Eiler, J.M., 2011. Formation of dolomite at 40–80 °C in the Latemar carbonate buildup, Dolomites, Italy, from clumped isotope thermometry. Geology 39 (6), 571–574.
Finnegan, S., Bergmann, K., Eiler, J.M., Jones, D.S., Fike, D.A., Eisenman, I., Hughes, N.C., Tripati, A.K., Fischer, W.W., 2011. The magnitude and duration of Late Ordovician–Early Silurian glaciation. Science 331 (6019), 903–906.
Friedman, I., O'Neil, J.R., 1977. Compilation of stable isotope fractionaction factors of geochemical interest, USGS Professional Paper 440-KK.
Ghosh, P., Adkins, J., Affek, H., Balta, B., Guo, W., Schauble, E.A., Schrag, D., Eiler, J.M., 2006. 13C–18O bonds in carbonate minerals: A new kind of paleothermometer. Geochim. Cosmochim. Acta 70 (6), 1439–1456.
Guo, W., Mosenfelder, J.L., Goddard, W.A., Eiler, J.M., 2009. Isotopic fractionations associated with phosphoric acid digestion of carbonate minerals: Insights from first-principles theoretical modeling and clumped isotope measurements. Geochim. Cosmochim. Acta 73 (24), 7203–7225.
Hampson, G.J., Howell, J.A., Flint, S.S., 1999. A sedimentological and sequence stratigraphic re-interpretation of the upper Cretaceous prairie canyon member ("Mancos B") and associated strata, Book Cliffs area, Utah, USA. J. Sediment. Res. 69 (2), 414–433.
Henkes, G.A., Passey, B.H., Wanamaker, A.D., Grossman, E.L., Ambrose, W.G., Carroll, M.L., 2013. Carbonate clumped isotope compositions of modern marine mollusk and brachiopod shells. Geochim. Cosmochim. Acta 106, 307–325.
Hudson, J.D., Coleman, M.L., Barreiro, B.A., Hollingworth, N.T.J., 2001. Septarian concretions from the Oxford Clay (Jurassic, England, UK): involvement of original marine and multiple external pore fluids. Sedimentology 48, 507–531.
Huntington, K.W., Eiler, J.M., Affek, H.P., Guo, W., Bonifacie, M., Yeung, L.Y., Thiagarajan, N., Passey, B., Tripati, A., Daeron, M., Came, R., 2009. Methods and limitations of 'clumped' CO2 isotope (Delta47) analysis by gas-source isotope ratio mass spectrometry. J. Mass Spectrom. 44 (9), 1318–1329.
Huntington, K.W., Budd, D.A., Wernicke, B.P., Eiler, J.M., 2011. Use of clumped-isotope thermometry to constrain the crystallization temperature of diagenetic calcite. J. Sediment. Res. 81 (9), 656–669.
Irwin, H., Curtis, C., Coleman, M., 1977. Isotopic evidence for source of diagenetic carbonates formed during burial of organic-rich sediments. Nature 269 (5625), 209–213.
Johnson, R.C., Nuccio, V.F., 1993. Surface vitrinite reflectance study of the Uinta and Piceance basins and adjacent areas, eastern Utah and western Colorado – implications for the development of laramide basins and uplifts. U.S. Department of the Interior, U.S. Government Printing Office.
Kenward, P.A., Goldstein, R.H., Gonzalez, L.A., Roberts, J.A., 2009. Precipitation of low-temperature dolomite from an anaerobic microbial consortium: The role of methanogenic Archaea. Geobiology 7 (5), 556–565.
Kim, S., Mucci, A., Taylor, B., 2007. Phosphoric acid fractionation factors for calcite and aragonite between 25 and 75 °C: Revisited. Chem. Geol. 246 (3–4), 135–146.
Klein, J.S., Mozley, P., Campbell, A., Cole, R., 1999. Spatial distribution of carbon and oxygen isotopes in laterally extensive carbonate-cemented layers: Implications for mode of growth and subsurface identification. J. Sediment. Res. 69 (1), 184–201.
Land, L.S., 1980. The isotopic and trace element geochemistry of dolomite: the state of the art. In: Zenger, D.H., Dunham, J.B., Ethington, R.L. (Eds.), Concepts and Models of Dolomitization. In: Society of Economic Paleontologists and Mineralogists Special Publication, vol. 38, pp. 87–110.
Lawrence, J.R., Gieskes, J.M., 1981. Constrains on the water transport and alteration in the oceanic crust from isotopic composition of pore water. J. Geophys. Res. 86, 7924–7934.
Lawrence, J.R., Taviani, M., 1988. Extreme hydrogen, oxygen and carbon isotope anomalies in the pore waters and carbonates of the sediments and basalts from the Norwegian Sea: methane, and hydrogen from the mantle?. Geochim. Cosmochim. Acta 52, 2077–2083.
Lawrence, J.R., Dreyer, J.I., Anderson, T.F., Brueckner, H.K., 1979. Importance of alteration of volcanic material in the sediments of Deep Sea Drilling site 323: chemistry, 180/1.0 and 87/86Sr. Geochim. Cosmochim. Acta 43, 573–588.

Loyd, S.J., Corsetti, F.A., Eiler, J.M., Tripati, A.K., 2012. Determining the diagenetic conditions of concretion formation: Assessing temperatures and pore waters using clumped isotopes. J. Sediment. Res. 82 (12), 1006–1016.
Machemer, S.D., Hutcheon, I., 1988. Geochemistry of early carbonate cements in the Cardium Formation, central Alberta. J. Sediment. Petrol. 58 (1), 136–147.
Malone, M.J., Claypool, G., Martin, J.B., Dickens, G.R., 2002. Variable methane fluxes in shallow marine systems over geologic time: the composition and origin of pore waters and authigenic carbonates on the New Jersey shelf. Mar. Geol. 189, 175–196.
McBride, E.F., Picard, M.D., Milliken, K., 2003. Calcite-cemented concretions in Cretaceous sandstones Wyoming and Utah, U.S.A. J. Sediment. Petrol. 73 (3), 462–483.
Mozley, P., 2002. Diagenetic structures. In: Middleton, G. (Ed.), Encyclopedia of Sediments and Sedimentary Rocks. Kluwer Academic Press, pp. 219–225.
Mozley, P.S., 1989. Complex compositional zonation in concretionary siderite – implications for geochemical studies. J. Sediment. Petrol. 59 (5), 815–818.
Mozley, P.S., 1996. The internal structure of carbonate concretions in mudrocks: A critical evaluation of the conventional concentric model of concretion growth. Sediment. Geol. 103 (1–2), 85–91.
Mozley, P.S., Burns, S.J., 1993. Oxygen and carbon isotopic composition of marine carbonate concretions – an Overview – Reply. J. Sediment. Petrol. 63 (5), 1008.
Mozley, P.S., Davis, J.M., 2005. Internal structure and mode of growth of elongate calcite concretions: Evidence for small-scale, microbially induced, chemical heterogeneity in groundwater. Geol. Soc. Am. Bull. 117 (11), 1400.
Nuccio, V.F., Roberts, R.N.L., 2003. Thermal maturity and oil and gas generation history of petroleum systems in the Uinta-Piceance Province, Utah and Colorado. In: Petroleum Systems and Geological Assessment of Oil and Gas in the Uinta-Piceance Province, Utah and Colorado. USGS Uinta-Piceance Assessment Team. Chapter 4.
Passey, B.H., Henkes, G.A., 2012. Carbonate clumped isotope bond reordering and geospeedometry. Earth Planet. Sci. Lett. 351–352, 223–236.
Quade, J., Eiler, J., Daëron, M., Achyuthan, H., 2013. The clumped isotope geothermometer in soil and Paleosol carbonate. Geochim. Cosmochim. Acta 105, 92–107.
Raiswell, R., Fisher, Q.J., 2000. Mudrock-hosted carbonate concretions: A review of growth mechanisms and their influence on chemical and isotopic composition. J. Geol. Soc. 157, 239–251.
Rosenbaum, J., Sheppard, S.M.F., 1986. An isotopic study of siderites, dolomites and ankerites at high temperatures. Geochim. Cosmochim. Acta 50, 1147–1150.
Scasso, R., Kiessling, W., 2001. Diagenesis of Upper Jurassic concretions from the Antarctic Penninsula. J. Sediment. Petrol. 71 (1), 88–100.
Schauble, E.A., Ghosh, P., Eiler, J.M., 2006. Preferential formation of C-13–O-18 bonds in carbonate minerals, estimated using first-principles lattice dynamics. Geochim. Cosmochim. Acta 70 (10), 2510–2529.
Shackleton, N.J., Kennett, J.P., 1975. Palaeotemperature history of the Cenozoic and the initiation of Antarctic glaciation. Oxygen and carbon isotope analysis in DSDP sites 277, 279 and 281.
Spinelli, G.A., Mozley, P.S., Tobin, H.J., Underwood, M.B., Hoffman, N.W., Bellew, G.M., 2007. Diagenesis, sediment strength, and pore collapse in sediment approaching the Nankai Trough subduction zone. Geol. Soc. Am. Bull. 119 (3–4), 377–390.
Swanson, E.M., Wernicke, B.P., Eiler, J.M., Losh, S., 2012. Temperatures and fluids on faults based on carbonate clumped-isotope thermometry. Am. J. Sci. 312 (1), 1–21.
Thyne, G.D., Boles, J.R., 1989. Isotopic evidence for origin of the Moeraki septarian concretions, New Zealand. J. Sediment. Petrol. 59, 272–279.
Vasconcelos, C., McKenzie, J.A., Warthmann, R., Bernasconi, S.M., 2005. Calibration of the δ18O paleothermometer for dolomite precipitated in microbial cultures and natural environments. Geology 33 (4), 317.
Wacker, U., Fiebig, J., Schoene, B.R., 2013. Clumped isotope analysis of carbonates: comparison of two different acid digestion techniques. Rapid Commun. Mass Spectrom. 27 (14), 1631–1642.